

**Evaluation of energy-distribution of a hybrid microbial fuel cell - membrane
bioreactor (MFC-MBR) for cost-effective wastewater treatment**

Jie Wang^{a,b,*}, Fanghua Bi^{a,b}, Huu-Hao Ngo^c, Wenshan Guo^c, Hui Jia^a, Hongwei Zhang^a
and Xinbo Zhang^d

^a State Key Laboratory of Separation Membranes and Membrane Processes,

Tianjin Polytechnic University, Tianjin 300387, China. E-mail:

wangjie@tjpu.edu.cn; Fax: +86 022 8395 5668; Tel.: +86 022 8395 5668

^b School of Environmental and Chemical Engineering, Tianjin Polytechnic

University, Tianjin 300387, China

^c Centre for Technology in Water and Wastewater, School of Civil and

Environmental Engineering, University of Technology Sydney, Sydney, NSW

2007, Australia

^d School of Environmental and Municipal Engineering, Tianjin Chengjian

University, Tianjin 300384, China

ABSTRACT

A low-cost hybrid system integrating a membrane-less microbial fuel cell (MFC) with an anoxic/oxic membrane bioreactor (MBR) was studied for fouling mitigation. The appended electric field in the MBR was supplied by the MFC with continuous flow. Supernatant from an anaerobic reactor with low dissolved oxygen was used as feed to the MFC in order to enhance its performance compared with that fed with synthetic wastewater. The voltage output of MFC maintained at 0.52 ± 0.02 V with 1000Ω resistor. The electric field intensity could reach to 0.114 V cm^{-1} . Compared with the conventional MBR (CMBR), the contents rather than the components of foulants on the cake layer of fouled MFC-MBR system was significantly reduced. Although only 0.5% of the feed COD was translated into electricity and applied to MBR, the hybrid system showed great feasibility without additional consumption but extracting energy from waste water and significantly enhancing the membrane filterability.

Keywords: membrane bioreactor; microbial fuel cell; membrane fouling; electric field; energy-distribution.

Introduction

Membrane bioreactor (MBR) combining the widely used activated sludge treatment with membrane separation offers several advantages over conventional activated sludge system such as stable and high effluent quality, small footprint and stricter discharge standards (Yu et al. 2014). Thus, MBRs are experiencing unprecedented growth for wastewater treatment and water reuse. However, the problem of membrane fouling limits MBR implementations (Akamatsu et al., 2010). Membrane fouling occurs with the interactions between the activated sludge mixed liquor and membrane material (Ji et al. 2008), and it is greatly associated with the physicochemical characteristics of activated sludge (Meng et al. 2006a). Many researchers have identified soluble microbial products (SMP) and extracellular polymeric substances (EPS) as the most significant biological factors leading to membrane fouling (Hong et al. 2014; Long et al. 2009). Furthermore, it has been reported that the foulants including sludge, SMP and EPS were negatively charged (Comerton et al., 2005). Therefore, electrophoresis forces could be conducive to reduce the deposition of particles onto the membrane surface. An earlier study by Sarkar et al. (2008) demonstrated that high voltage electric field applied to cross-flow ultrafiltration could suppress membrane fouling and enhance the permeate flux. In another study, lower electric intensity was used to mitigate membrane fouling through sludge modification (Liu et al., 2012). Bani-melhem and Elektorowicz (2010) also reported that an even low electric intensity (1 V/cm, on and off) could reduce membrane fouling (by 16%) and improve the sludge filterability. Liu [9] demonstrated

that the minute electric field (0.036 V/cm and 0.073 V/cm) repulsed the negatively charged particles from the membrane surface and modified the sludge properties, thereby lowering membrane fouling rate.

Microbial fuel cells (MFCs) are a promising technology which is clean, renewable and non-pollution (Min, B et al., 2005). However, the effluent quality of MFC is generally insufficient to meet the strict effluent requirement with limited biomass retention. Therefore, Wang et al. (2013) proposed a MFC-MBR integrated process using the aeration tank of a MBR as cathode chamber, in which the anodic chamber was filled with self-fabricated activated carbon fiber and directly submerged in the membrane bioreactor. The performance of power generation and wastewater treatment were investigated but without the investigation of membrane fouling. Although some suggestions (Su et al., 2013; Tian et al., 2014) about combining MBR with MFC have been proposed for simultaneously membrane fouling mitigation and energy recovery, the application of the generated power was neglected. Tian et al. (2015) developed an integrated MFC-MBR system using the electric field between two electrodes to improve wastewater treatment and mitigate membrane fouling. However, this construction is impractical. Hence, a novel MFC-MBR (EMBR) combined system was proposed based on the widely used membrane module configuration. Furthermore, a membrane-less MFC with continuous inflow was applied to reduce the construction cost. But dissolved oxygen (DO) was regarded as a fatal factor for such a MFC without proton exchange membrane (PEM) which was used to prevent oxygen diffusion from cathode to anode (Fan et al., 2007). Hence, the

influent water of MFC was replaced by supernatant of anaerobic reactor with low dissolved oxygen in order to enhance the electricity generation performance.

In this study, a novel low-cost hybrid system combining MFC and MBR (MFC-MBR) was developed based on the practical application. The influent of MFC was supernatant of an anaerobic reactor with low dissolved oxygen. And the voltage generated by MFC was appended to the installed electrodes in MBR to reduce the energy consumption of a DC power. Three operational cycles were repeated to compare the performance of two systems. Electrophoresis and electrostatic repulsion against electronegative colloids or particles were particularly explained to fouling reduction. And activated sludge modification was investigated to further explore the mechanisms of membrane fouling reduction in the MFC-MBR.

2. Materials and methods

2.1 Integrated MFC-MBR system

As shown in Fig.S1, the MFC-MBR system was constructed with an anoxic/oxic membrane reactor and an air-cathode MFC. The effective volumes of each group of anoxic tank and oxic tank were 3.5 L (10cm×10cm×35cm) and 6.5 L (10cm×12cm×54cm), respectively. The effective filtration area of PVDF hollow fiber membrane (pore size 0.22μm, Tianjin Motimo Membrane Technology Co., Ltd., China) was 0.1 m². In the oxic tank of the MFC-MBR system, two graphitic plates (20cm×10cm×0.3cm) were placed on the opposite side of the reactor as anode, while a graphitic rod (diameter 0.6 cm, length 20 cm) was fastened in the center of the

membrane module as cathode. A conventional MBR (CMBR) was running as a control experiment.

The MFC was constructed using plexiglas. Its effective volume (10 cm×10 cm×10 cm) was 0.88 L. The anode was three pieces of carbon felts (384 cm², Beijing Fengxiang Technology Co., Ltd., China) without any pretreatment. The carbon cloth cathode was coated with four diffusion layers to prevent water loss according to previous research by Liu et al., (2008). Pt loading of 0.5 mg/cm² was employed using a Nafion solution (5%) as a catalyst binder and the coated cathode was dried for 1 day at room temperature before use. As no PEM (proton exchange membrane) was used, the production cost was reduced greatly. Two electrodes were connected through a 1000Ω resistor. The cell voltage was recorded automatically every 15 min using a multimeter. The influent flow rate of anode chamber was 0.14 L/h using a peristaltic pump (BT100-2J, Baoding Longer Precision Pump Co., Ltd., China), and the hydraulic retention time (HRT) was about 6.3 h.

2.2 Operating conditions

The feed water was synthetic wastewater, containing 272 mg/L of glucose, 272 mg/L of starch, 305 mg/L of NaHCO₃, 145 mg/L of (NH₄)₂SO₄, 40 mg/L of urea, 18.5 mg/L of KH₂PO₄, 23.5 mg/L of K₂HPO₄, 23.5 mg/L of MgSO₄·7H₂O, 14.4 mg/L of CaCl₂, 21 mg/L of FeSO₄·7H₂O, and 0.32 mg/L of MnSO₄·4H₂O (Su et al., 2013). The activated sludge was taken from Jizhuangzi Wastewater Treatment Plant (Tianjin, China). Two MBRs were operated at the same condition for comparison. The

membrane flux was maintained at $7.5 \text{ L}/(\text{m}^2 \cdot \text{h})$ using a peristaltic pump with an intermittent suction of 8 min “on” and 2 min “off” controlled by the programmable logic controller (PLC, SIEMENS, Germany). The DO concentration was maintained at 2-4 mg/L with the aeration rate at $0.2 \text{ m}^3/\text{h}$. Mixed liquid suspended solids (MLSS) concentrations of two MBRs were maintained at the same level, about 3158 ± 216 mg/L. The sludge returned from oxic tank to anoxic tank every 2 h for 10 min and the reflux ratio was 100%. The trans-membrane pressure (TMP) was measured using a pressure sensor (MBS 3000, Danfoss, Denmark) with a paperless recorder.

2.3 Analytical methods

During the operation, the concentrations of MLSS, MLVSS, ammonia and Chemical Oxygen Demand (COD) were measured according to the standard method (APHA, 1995). The particle size distribution of activated sludge was measured using Malvern Mastersizer 2000 (Malvern Instruments, UK), and the zeta potential (ZP) was determined using Zetasizer Nano 1000 (Malvern Instruments, UK). The activated sludge floc was broken into small particles by shaking and the supernatant was sampled 10 min afterwards for zeta potential measurement (Chang et al., 2001). The functional groups of foulants were analyzed by fourier transform infrared spectroscopy (FTIR) (NICOLET6700, Thermo Fisher, Massachusetts, USA). The SMP and EPS were extracted by centrifugation-filtration and heating method (Tian et al., 2014) and analyzed for the contents of protein and carbohydrate. The sum of carbohydrate (EPS_c) and protein (EPS_p) was regarded as the total EPS concentration

(EPS_t). The fluorescence excitation emission matrix (EEM) spectroscopy of SMP and EPS were detected by fluorescence spectrophotometer (F-7000, Hitachi, Tokyo, Japan). Moreover, samples were filtered through a microfiltration membrane (0.45 μm) prior to analysis.

The polarization curve of MFC was obtained by varying the circuit external resistance from 9999 to 5 Ω when the cell voltage was relatively stable. Coulombic efficiency (CE) of MFC was calculated as $CE = C_p/C_t \times 100\%$, where C_p is the total coulombs calculated by integrating the current over time, and C_t is the theoretical amount of coulombs available based on COD removed in the MFC (Wang et al., 2013).

3. Results and discussion

3.1 Electricity generation performance

Fig. 1

The MFC was incubated with synthetic wastewater at an external resistance of 1000Ω. With the anaerobic sludge injected, the voltage output of MFC became stable at 0.44 ± 0.02 V (from 0.11 V) within a short start-up period (about 100h). And power density polarization curves were then measured (Fig. 1b and c). The open circuit voltage of the MFC was 0.49 V and the maximum power density was 0.045 W/m^2 (normalized to the cathode area). It could be easily calculated that the internal resistance of the MFC was about $150 \pm 25 \Omega$ according to the slope. During the following steady state, the coulombic efficiency (CE) was calculated as 3.87%. The

lower CE was also attributed to the oxygen diffusion from cathode to anode (Fan et al. 2007). As membrane was used to reduce the oxygen diffusion in the air-cathode MFC, DO was inferred to be a fatal factor for a membrane-less MFC in this study. After changing to the supernatant of an anoxic reactor, the voltage kept stable for about 10 days. From Fig. 1a, it could be obviously observed that the voltage output of MFC increased to $0.52\pm 0.02\text{V}$ rapidly after varying the substrates (from the synthetic wastewater to supernatant of an anoxic reactor). The power density polarization curves were measured again. The open circuit voltage was 0.66 V with maximum power density of 0.059 W/m^2 , and the internal resistance and CE were about $150\pm 25\Omega$ and 8.56%, respectively. Both power density and CE were enhanced by changing inflow water with low DO, especially for CE, which is over 100% higher than the MFC feed with synthetic wastewater, confirming the dominating factor of DO in power output and CE limitation. Thus, further improvements in performance of MFC could be made significantly just through altering feed water with the same configuration. And this was easy to achieve in this hybrid system.

3.2 Evaluation of impact on MBR with the electric field generated by continuous

MFC

3.2.1 Electric field intensity

After the voltage kept stable for about 10 days, the 1000Ω resistance was replaced by electrodes in MBR. Two graphitic plates were connected to the bio-cathode of MFC through copper wire, while the graphitic electrode was connected

to the anode of MFC. After that the voltage rose to a higher level (0.57 ± 0.05 V).

Thousands of load resistance between two electrodes in MBR could be deduced based on the polarization curve. The electric field intensity was calculated to be about 0.114 V cm^{-1} as the distance between two electrodes was close to 5 cm, which was large enough compared with previous study reported (Liu et al, 2012). New membrane modules were installed until two systems have been operated stably. Then the TMP increase of two systems were recorded and detailed investigations were carried out.

3.2.2 Membrane fouling of the MFC-MBR and CMBR

Fig.2

As an important parameter reflecting membrane filtration efficiency in MBR systems, TMP is used to evaluate the membrane fouling condition. Two membranes were under the same constant flux operation $7.5\text{ L}/(\text{m}^2\text{h})$ throughout the entire operation of 38 days. TMP variations are illustrated in Fig. 2. Obviously, TMP increased slowly at beginning, potentially due to the attachment of organic matter. Then, the TMP of CMBR increased rapidly, whereas the TMP development of MFC-MBR exhibited considerably slower increase. When the TMP of CMBR reached up to 40 kPa on day 18, 30 and 38, the TMP of MFC-MBR only reached 21 kPa, 20 kPa and 17 kPa, respectively. Physical cleaning was applied to remove membrane foulants for both membranes, and they were performed three cleaning cycles. Compared with the virgin membrane, the fouling rate increased more rapidly after physical cleaning. This change in fouling rate indicated that the membrane could not

be completely recovered through physical cleaning, and it was easier for foulants to attach on the remained fouling layer (Tian et al., 2015). It was observed that significant membrane fouling mitigation occurred with the equipment of electric field in MFC-MBR, indicating the weak electric field was effective to maintain the electrophoresis and electrostatic attraction/repulsion against electronegative sludge particles or colloids.

FTIR spectra were primarily used to identify the functional groups in compounds. In order to further explore the foulants responsible for membrane pore blocking, FTIR analysis was conducted on both clean and fouled membrane at the end of each cycle. In the spectra, the peaks at 3276 cm^{-1} (O-H stretch) and 2922 cm^{-1} (C-H stretch) indicate the presence of carbohydrate-like substances. And the spectrum intensity observed in the CMBR is higher compared with that in the MFC-MBR. Same tendency peaks at 1637 cm^{-1} (C=O stretch) and 1542 cm^{-1} (N-H in-plane bending) are protein structure: amides \square and amides \square . Thus, it could be inferred that protein and carbohydrate are the dominant membrane foulants in fouled membrane from the FTIR spectrum. Similar results were also reported by Kim and Jang (Kim and Jang, 2006). In addition, higher spectrum intensity in the peak of CMBR was observed, showing that the concentrations of both protein and carbohydrate were reduced by appending electric field as it could reduce the deposition rate of foulants. The similar spectra from 1800 cm^{-1} to 2500 cm^{-1} and from 400 cm^{-1} to 1500 cm^{-1} between fouled MFC-MBR and clean membrane might be ascribed to the membrane material themselves. However, significant differences of spectra from 400 cm^{-1} to 1500 cm^{-1}

between CMBR and clean membrane could be observed. The spectrums from 600 cm^{-1} to 900 cm^{-1} were indicative of humic substances (Tran et al. 2007). The peaks in the range of 1000-1500 cm^{-1} indicated the presence of both protein and carbohydrate. Hence, it could be inferred that more foulants including protein, carbohydrate and humic substances existed in the fouled CMBR so as to that the intrinsic peaks of clean membrane were covered, which was verified by the FTIR spectra of washed membrane and fresh membrane. After physically cleaning, most of foulants were eliminated and similar peaks could be observed for both washed membranes from two systems and fresh membrane in the FTIR spectra.

3.2.3 Mechanisms of membrane fouling mitigation

Table 1

In order to further investigate the components of cake layer of fouled membranes of CMBR and MFC-MBR, the SMP and EPS from cake layer were extracted and analysed for that they have been reported as the predominant cause of membrane fouling containing mainly protein and carbohydrate (Duan et al., 2014). As shown in Table 1, an alleviated concentrations of SMP_c (23.17%) and EPS_c (11.42%) in membrane cake layer was observed in the MFC-MBR system. However, less correlation existed between the protein and membrane fouling of two systems. Comparatively, the contents of protein and carbohydrate both decreased effectively in the MFC-MBR through TMP and FTIR analysis. It elucidated that the appended electric field could effectively reduce the deposition rate of foulants, while the components of foulants on two fouled membranes were almost the same except for a

slight difference of carbohydrate.

Thus, the components of SMP and EPS in mixed liquor of two bioreactors were also investigated so as to reveal the causes of membrane fouling mitigation resulting from electric field. Obviously, a quite lower SMP/EPS ratio in mixed liquor and a relatively higher SMP/EPS ratio in cake layer were observed (Fig S2), which indicated that SMP was a more crucial factor for sludge cake formation and leading to severe membrane fouling compared with EPS. Furthermore, although similar protein concentrations are presented in the mixed liquors of two systems, the concentration of SMP in mixed liquor of MFC-MBR decreased by 21.14% due to the application of electric field, especially for carbohydrate. A relatively higher SMP_p/SMP_c ratio of 1.011 was observed. It has been reported that the metabolism activity of microorganisms could be enhanced by the electric field (Bani-melhem and Elektorowicz, 2010) and carbohydrate can be utilized as carbon and energy sources by bacteria with substrate shortage (Sheng, et al., 2010). Therefore, the decrease of SMP_c in the mixed liquor resulted in the decrease of carbohydrate in the cake layer of EMBR system. For EPS, it could be reduced by 12.28% with the equipped electric field. Unlike SMP, both EPS_p and EPS_c decreased and no statistical difference in EPS_p/EPS_c ratio of the mixed liquor was observed between two systems. Similarly, the decrease of EPS_c in the mixed liquor led to the decrease of carbohydrate in the cake layer. However, the same concentrations of EPS_p between two fouled membranes could partly be attributed to the secretion of the microorganisms attaching on the membrane surface.

Fig. 3

The zeta potential of sludge in aeration tank of MFC-MBR and CMBR averaged at -18.2 and -22.8, respectively, confirming the theory that zeta potential mainly results from the change of EPS concentration, and they are in inverse proportion (Meng et al., 2006b). According to the Derjaguin, Landau, Verwey and Overbeek (DLVO) theory (Azeredo et al., 1999), sludge suspension with low zeta potential (absolute value) has a strong aggregation tendency. Fig. 3 delineates the PSD measurement carried out at the end of operation. It could be observed that a slight shift to large flocs compared with the CMBR. Furthermore, the particles having a size smaller than 50 μm were significantly reduced by 37.4%, leading to greater specific and cake resistance (Bai and Leow, 2002). These results clearly showed that the applied electric field played a crucial role to enhance sludge aggregation.

Three-dimensional EEM fluorescence spectra were adopted to compare the components of SMP and EPS in oxic bioreactors of two systems (Fig S3). Four main peaks could be identified for SMP from Fig S3. The peaks located at excitation/emission (Ex/Em) 230/340 nm, 235/385 nm, 275/330 nm and 350/410 nm were described as simple aromatic proteins (peak A), fulvic acid-like materials (peak B), soluble microbial byproduct-like material (peak C) and humic acid-like organics (peak D), respectively (Wen et al. 2003). The fluorescent intensities of four peaks, especially for fulvic acid-like materials (peak B) and humic acid-like organics (peak D) in SMP were significantly weakened after applying electric field. For EPS, three peaks (A, C and D) could be observed, and all of them were weaker in MFC-MBR

compared with those in CMBR. Particularly, the humic acid-like organics (peak D) were reduced significantly. Furthermore, the location of the peak D of EPS demonstrated a blue-shift, indicating the large molecules in humic acid-like organics were broken into smaller fragments under the metabolism of modified activated sludge. Therefore, the protein, carbohydrate and humic acid-like organics of SMP and EPS were significantly decreased simultaneously, resulting in the lower deposition rate of foulants and membrane fouling mitigation.

3.3 Mass balances of COD in the EMBR

Fig. 4

The mass balances of COD were analyzed to further insight into the allocations of energy in the whole hybrid system. And the procedures for all calculations were listed in the supplementary document. Raw water with $620 \pm 45 \text{ mg L}^{-1}$ COD was fed into the anoxic tank. The TCOD in the influent was 11160 mg d^{-1} based on calculation (with permeate flux $7.5 \text{ L m}^{-2} \text{ h}^{-1}$). After anaerobic digestion, $287 \pm 23 \text{ mg L}^{-1}$ COD was left in the supernatant, and the average COD removal efficiency for the anoxic reactor was 53.71%. The average COD removal capacity was then calculated to be 5994 mg d^{-1} , most of which flowed into oxic tank except a small part flowed into the MFC. The COD in the effluent was $38 \pm 6 \text{ mg L}^{-1}$, indicating the non-degraded COD was about 684 mg d^{-1} . The average COD removal capacity was about 4482 mg d^{-1} in the oxic tank and MFC, containing aerobic digestion (3864 mg d^{-1}) in oxic tank, anaerobic digestion (565 mg d^{-1}) as well as electricity generation process in MFC (53 mg d^{-1}). Thus, it could be inferred that only about 0.5% energy of the sewage in the

whole system turned to be electricity. Though a small proportion of COD consumption was related to electricity process, the electric field played a significant role on the membrane fouling mitigation. This hybrid system showed great feasibility without additional consumption but extracting energy from waste water and significantly enhancing the membrane filterability.

4. Conclusion

In this study, cost-effective materials were adopted for a hybrid MFC-MBR system. With the supernatant from anoxic reactor as feed to the membrane-less MFC, the electric field intensity could reach to 0.114V cm^{-1} after it was appended to the MBR. Membrane fouling mitigation could be observed in the hybrid system by reducing the deposition rate of foulants. SMP and EPS were significantly decreased simultaneously. The applied electric field played a crucial role to enhance sludge aggregation. This hybrid system showed great feasibility without additional consumption but extracting energy from waste water and significantly enhancing the membrane filterability.

Acknowledgements

This study was financially supported by the National Natural Science Foundation of China (No. 51578375, 51378349), China Postdoctoral Science Foundation (2013M541184), and Program for Changjiang Scholars and Innovative Research Team in University of Ministry of Education of China (Grand No. IRT13084).

References

1. Akamatsu, K., Lu, W., Sugawara, T., Nakao, S.-I., 2010. Development of a novel fouling suppression system in membrane bioreactors using an intermittent electric field. *Water Res.* 44, 825-830.
2. APHA, 1998. Standard methods for the examination of water and wastewater. American Public Health Association, Washington, DC.
3. Azeredo, J., Visser, J., Oliveira, R., 1999. Exopolymers in bacterial adhesion: interpretation in terms of DLVO and XDLVO theories. *Colloids Surf. B-Biointerfaces.* 14, 141-148.
4. Bai, R., Leow, H.F., 2002. Microfiltration of activated sludge wastewater-the effect of system operation parameters. *Sep. Purif. Technol.* 29, 189-198.
5. Bani-melhem, K., Elektorowicz, M., 2010. Development of a novel submerged membrane electro-bioreactor (SMEBR): performance for fouling reduction. *Environ. Sci. Technol.* 44, 3298-3304.
6. Chang, G.R., Liu, J.C., Lee, D.J., 2001. Co-Conditioning and dewatering of chemical sludge and waste activated sludge. *Water Res.* 35, 786-794.
7. Comerton, A.M., Andrews, R.C., Bagley, D.M., 2005. Evaluation of an MBR-RO system to produce high quality reuse water: microbial control, DBP formation and nitrate. *Water Res.* 39, 3982-3990.
8. Duan L., Song Y.H., Yu H.B., Xia S.Q., Hermanowicz S.W., 2014. The effect of solids retention times on the characterization of extracellular polymeric

- substances and soluble microbial products in a submerged membrane bioreactor. *Biores Technol.* 163, 395-398.
9. Fan, Y.Z., Hu, H.Q., Liu, H., 2007. Enhanced Coulombic efficiency and power density of air-cathode microbial fuel cells with an improved cell configuration. *J Power Sources.* 171, 348-354.
10. Hong, H.C., Zhang, M.J., He, Y.M., Chen, J.R., Lin, H.J., 2014. Fouling mechanisms of gel layer in a submerged membrane bioreactor. *Biores Technol.* 166, 295-302.
11. Ji, J., Qiu, J.P., Wong, F.S., Li, Y.Z., 2008. Enhancement of filterability in MBR achieved by improvement of supernatant and floc characteristics via filter aids addition. *Water Res.* 42, 3611-3622.
12. Kim, S., Jang, N., 2006. The effect of calcium on the membrane biofouling in the membrane bioreactor (MBR). *Water Res.* 40 (14), 2756-2764.
13. Liu, H., Cheng, S.A., Huang, L.P., Logan, B.E., 2008. Scale-up of membrane-free single-chamber microbial fuel cells. *J Power Sources.* 179, 274-279.
14. Liu, L.F., Liu, J.D., Gao, B., Yang, F.L., 2012. Minute electric field reduced membrane fouling and improved performance of membrane bioreactor. *Sep. Purif. Technol.* 86, 106-112.
15. Long, G.Y., Zhu, P.T., Shen, Y., Tong, M.P., 2009. Influence of extracellular polymeric substances (EPS) on deposition kinetics of bacteria. *Environ. Sci. Technol.* 43, 2308-2314.
16. Meng F.G., Zhang H.M., Yang F.L., Li Y.S., Xiao J.N., Zhang X.W., 2006a. Effect

of filamentous bacteria on membrane fouling in submerged membrane bioreactor.

J. Membr. Sci. 272, 161-168.

17. Meng, F.G., Zhang, H.M., Yang, F.L., Zhang, S.T., Li, Y.S. Zhang, X.W., 2006b.

Identification of activated sludge properties affecting membrane fouling in submerged membrane bioreactors. *Sep. Purif. Technol.* 51, 95-103.

18. Min, B., Kim, J., Oh, S., Regan, J.M., Logan, B.E., 2005. Electricity generation

from swine wastewater using microbial fuel cell. *Water Res.* 39, 4961-4968.

19. Sarkar, B., Pal, S., Ghosh, T.B., De, S., Das, G.S., 2008. A study of electric field

enhanced ultrafiltration of synthetic fruit juice and optical quantification of gel deposition. *J. Membr. Sci.* 311, 112-120.

20. Sheng G.P., Yu H.Q., Li X.Y., 2010. Extracellular polymeric substances (EPS) of

microbial aggregates in biological wastewater treatment systems: a review, *Biotechnol. Adv.* 28, 882-894.

21. Su, X.Y., Tian, Y., Sun, Z.C., Lu, Y.B., Li, Z.P., 2013. Performance of a combined

system of microbial fuel cell and membrane bioreactor: Wastewater treatment, sludge reduction, energy recovery and membrane fouling. *Biosens. Bioelectron.*

49, 92-98.

22. Tian, Y., Ji, C., Wang, K., Le-Clech, P., 2014. Assessment of an anaerobic

membrane bio-electrochemical reactor (AnMBER) for wastewater treatment and energy recovery. *J. Membr. Sci.* 450, 242-248.

23. Tian, Y., Li, H., Li, X.Y., Su, X.Y., Lu, Y.B., Zuo, W., Zhang, J., 2015. In-situ

integration of microbial fuel cell with hollow-fiber membrane bioreactor for

- wastewater treatment and membrane fouling mitigation. *Biosens. Bioelectron.* 64, 189-195.
24. Tran T., Bolto B., Gray S., Hoang M., Ostarcevic E., 2007. An autopsy study of a fouled reverse osmosis membrane element used in a brackish water treatment plant. *Water Res.* 41,3915–3923.
25. Wang, J., Zheng, Y.W., Jia H., Zhang, H.W., 2013. In situ investigation of processing property in combination with integration of microbial fuel cell and tubular membrane bioreactor. *Biores Technol.* 149, 163-168.
26. Wang, Y.P., Liu, X.W., Li, W.W., Li, F., Wang, Y.K., Sheng, G.P., Roymand J. Zeng, Yu, H.Q.,2012. A microbial fuel cell-membrane bioreactor integrated system for cost-effective wastewater treatment. *Appl. Energ.* 98, 230-235.
27. Wen, C., Paul, W., Jerry, A.L., Karl, B., 2003. Fluorescence excitation-emission matrix regional integration to quantity spectra for dissolved organic matter., *Environ. Sci. Technol.* 37, 5701-5710.
28. Yu H.Y., Lin H.J., Zhang M.J., Hong Y.M., Wang F.Y., Zhao L.H., 2014. Membrane fouling in a submerged membrane bioreactor with focus on surface properties and interactions of cake sludge and bulk sludge. *Biores Technol.* 169, 213-219.

Figure Captions

Fig. 1 Variation of (a) voltage output with time; (b) power density and (c) polarization curves of MFC fed with different inflow

Fig.2 TMP profiles of the MFC-MBR and CMBR

Fig. 3 The size distributions of aerobic activated sludge flocs in the CMBR and MFC-MBR (the area of shadow zone indicates the difference value that the particles having a size smaller than 50 μm between two systems)

Fig. 4 Mass balances of COD in the MFC-MBR

ACCEPTED MANUSCRIPT

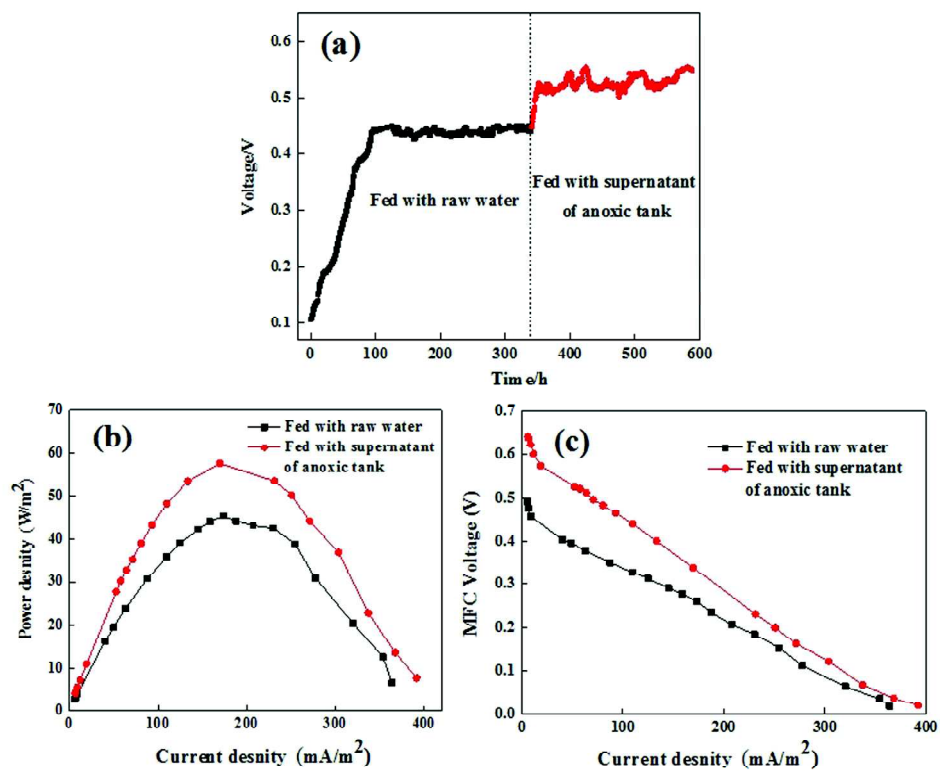


Fig. 1 Variation of (a) voltage output with time; (b) power density and (c) polarization curves of MFC fed with different inflow

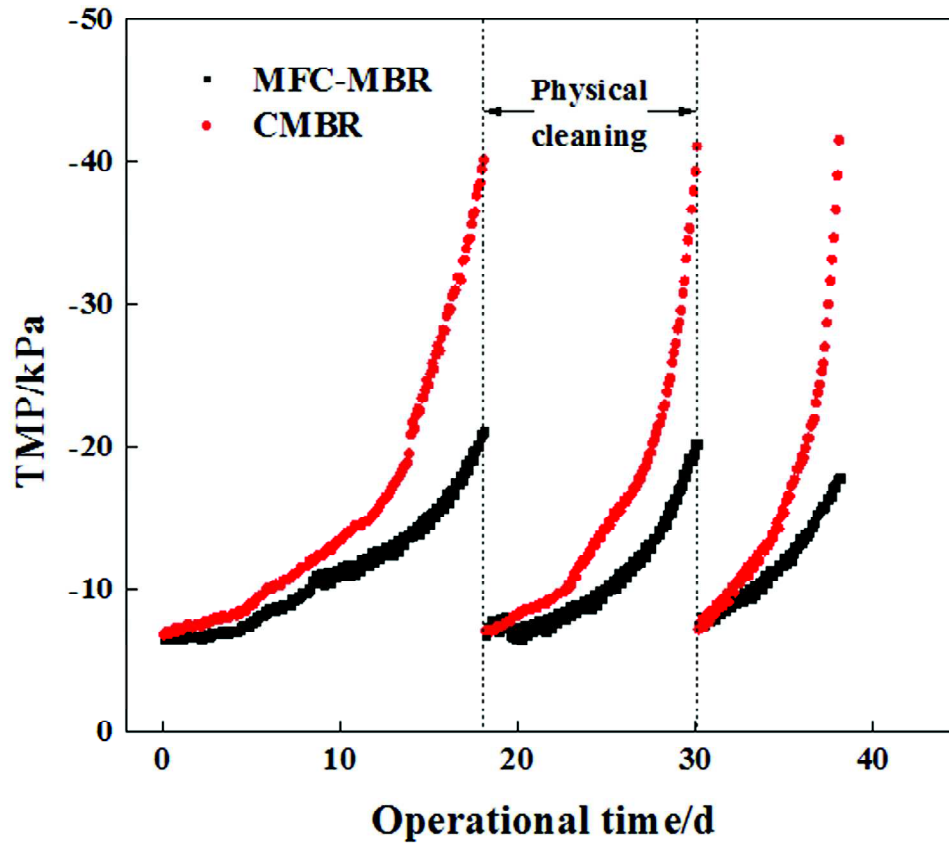


Fig.2 TMP profiles of the MFC-MBR and CMBR

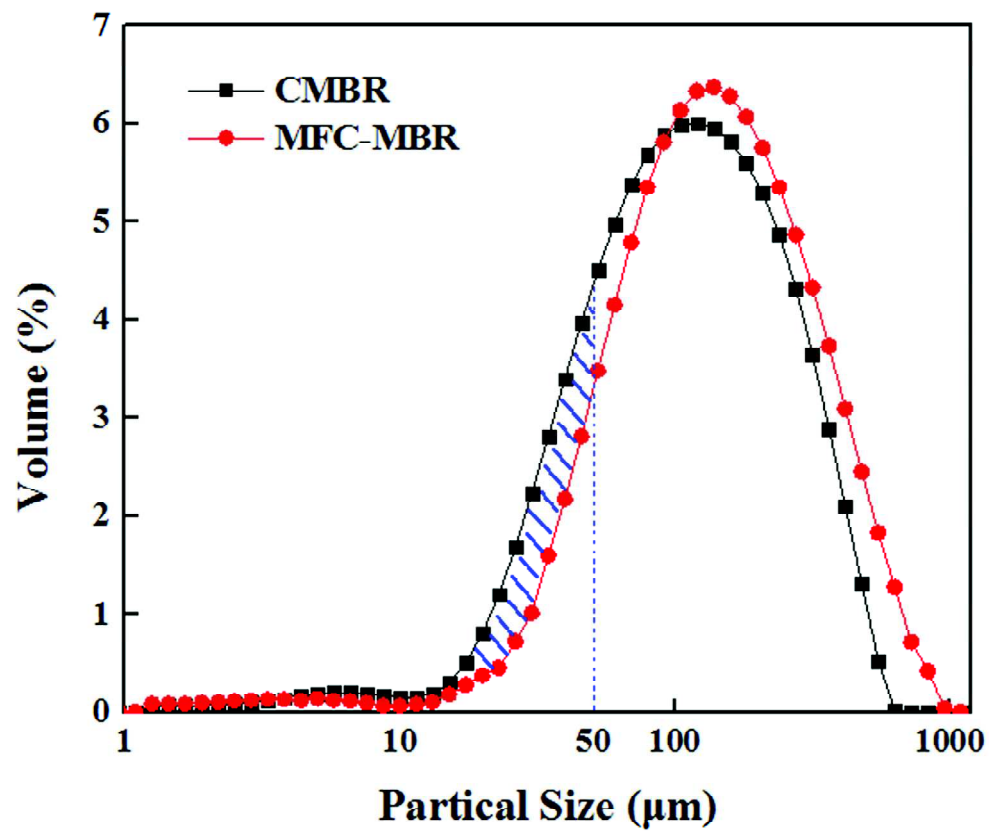


Fig. 3 The size distributions of aerobic activated sludge flocs in the CMBR and MFC-MBR (the area of shadow zone indicates the difference value that the particles having a size smaller than 50 µm between two systems)

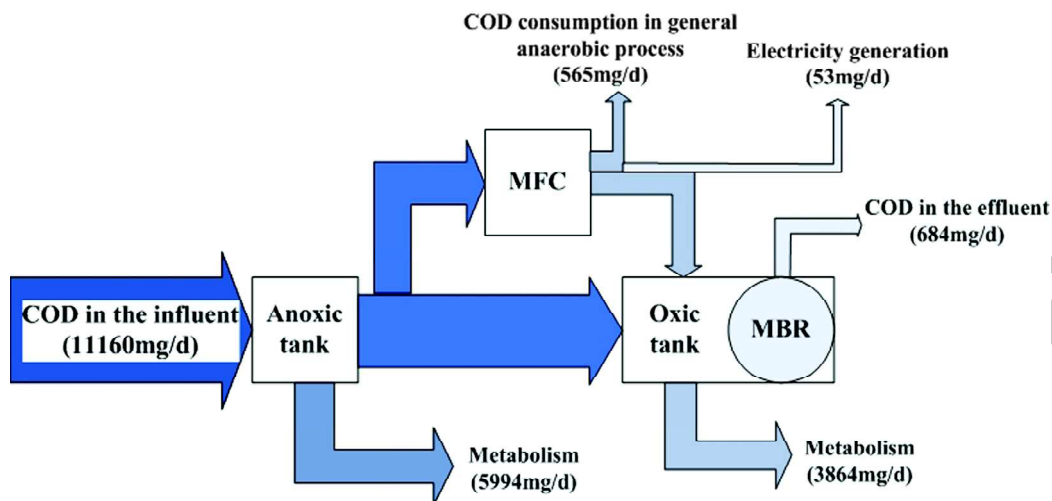


Fig. 4 Mass balances of COD in the MFC-MBR

Table 1The microbial products of mixed liquor and cake sludge in two systems^a

Items	CMBR		MFC-MBR	
	Mixed liquor	Cake layer	Mixed liquor	Cake layer
SMP (mg g ⁻¹ _{MLSS})	20.15±2.34	127.53±8.26	15.89±2.27	111.90±9.26
SMP _p	8.11±1.17	59.43±4.13	7.98±1.20	59.58±5.32
SMP _c	12.04±1.26	68.10±4.66	7.89±1.18	52.32±4.11
SMP _p /SMP _c	0.674±0.034	0.869±0.058	1.011±0.050	1.146±0.082
EPS(mg g ⁻¹ _{MLSS})	83.82±6.58	107.06±6.67	73.53±5.67	102.11±6.31
EPS _p	63.27±4.86	69.93±4.39	55.46±3.26	69.22±4.79
EPS _c	20.55±2.61	37.13±2.45	18.07±2.55	32.89±2.03
EPS _p /EPS _c	3.088±0.142	1.883±0.094	3.069±0.112	2.105±0.128
Zeta potential (mV)	22.8±0.4	-	18.2±0.3	-

^a Values within the table denote averages ± standard deviations.

Highlights

- A low-cost MFC-MBR system was established based on the membrane module configuration.
- The weak electric field generated by MFC could effectively mitigate membrane fouling.
- Low dissolved oxygen feed water increased the performance of membrane-less MFC.
- Energy-distribution of the combined system was evaluated.